Catalysis Today 156 (2010) 223–228

Contents lists available at ScienceDirect

Catalysis Today

journal homepage: www.elsevier.com/locate/cattod

Effect of flow configuration on the behavior of a membrane reactor operating without sweep gas

M.E. Adrover, A. Anzola, S. Schbib, M. Pedernera, D. Borio*

Planta Piloto de Ingeniería Química (PLAPIQUI), Universidad Nacional del Sur-CONICET, Camino La Carrindanga Km 7, 8000 Bahía Blanca, Argentina

ARTICLE INFO

Article history:
Available online 31 March 2010

Keywords:
Membrane reactor
WGS
Hydrogen production
Pd membrane

ABSTRACT

A simulation study of a multitubular membrane reactor for the water gas shift reaction is presented. No sweep gas is considered. Two alternative flow configurations between the retentate and permeate streams are compared: cocurrent and countercurrent. The influence of the flow scheme on the ignition temperatures, CO conversions and axial temperature profiles is analyzed. Simple algebraic equations are derived to predict the temperature rise along the reactor length.

The cocurrent scheme enables the attenuation of the thermal effects in the membrane reactor, by minimizing the temperature rise in the catalyst bed. Conversely, the temperature rise corresponding to the countercurrent scheme is considerably higher than that of the cocurrent configuration. Both thermal increases exceed the temperature rise of a conventional adiabatic fixed-bed reactor. Under countercurrent flow, the membrane reactor could exhibit steady-state multiplicity because of the heat feedback introduced by the permeate stream.

1. Introduction

The hydrogen production process and subsequent purification steps have been extensively studied in the last two decades for fuel-cell feeding. Hydrogen is industrially obtained from steam reforming of hydrocarbons or alcohols. In most cases, the CO content resulting from the reactor has to be reduced to avoid the poisoning of the fuel-cell anode catalyst. The water gas shift reaction (WGSR) is selected to accomplish this objective, with the additional effect of increasing the H_2 production:

$$CO + H_2O \leftrightarrow CO_2 + H_2 \qquad \Delta H^{\circ}_{298\,K} = -41.09\,kJ/mol \qquad (1)$$

As the WGSR is strongly limited by equilibrium, this reactor could become the biggest one of the generation–purification system [1]. An attractive alternative to the Fixed-Bed Reactor (FBR) is the Membrane Reactor (MR). A dense membrane (e.g., Pd–Ag supported on a porous substrate) is used to shift the equilibrium by means of selective permeation of one of the reaction products (e.g., H_2). The advantages of the MR to carry out reactions with equilibrium limitations have already been demonstrated [2,3]. In most of the literature, heat effects are neglected and the MR operation is assumed to be isothermal. This assumption is reasonable for low-scale (laboratory) reactors due to the high heat transfer area/reaction volume ratios under use. When there are several membrane tubes inside a shell, however, the hypothesis of isothermal operation could no longer be valid and thermal effects need to be evaluated [4,5].

In order to increase the permeation through the membrane, a sweep gas (e.g., N_2 or steam) is usually employed; this alternative, however, requires a separation stage downstream. An increase in the feed pressure on the reaction side leads to high permeation fluxes, in which case neither the sweep gas nor the consequent H_2 purification are necessary.

Brunetti et al. [6] studied the WGSR in a lab-scale MR operating without sweep gas, by means of a pseudohomogenous non-isothermal model. The authors analyzed the influence of the operating pressure on the MR behavior under a cocurrent scheme and introduced the concepts of volume and conversion indexes. Basile et al. [7] considered both flow configurations, i.e. cocurrent and countercurrent, for the WGS membrane reactor. They proposed a two-dimensional model to study the behavior of the MR operating with N_2 as sweep gas. Isothermal conditions were assumed.

The aim of the present work is to analyze the thermal effects of a multitubular membrane reactor for the WGSR, operating without sweep gas, under co- and countercurrent flow. The influence of the flow scheme on the reaction ignition and the CO conversion is analyzed. Simple algebraic equations to predict the temperature rise inside the catalyst bed are proposed.

* Corresponding author. Tel.: +54 291 4861700; fax: +54 291 4861600.
E-mail address: dborio@plapiqui.edu.ar (D. Borio).

0920-5861/$ – see front matter © 2010 Elsevier B.V. All rights reserved.
doi:10.1016/j.cattod.2010.02.035

Nomenclature

A_T	cross-sectional area of shell, m^2
C_{pj}	heat capacity of component j, kJ/(mol K)
C_p	$\sum y_{j,o}C_{pj}$ = heat capacity of reaction mixture, kJ/(mol K)
d	diameter of tube, m
E	activation energy, J/mol
F	molar flowrate, mol/s
J_{H_2}	permeation flow of H_2, mol/(s m^2)
k	kinetic constant, $mol_{CO}/(kg_{cat}\ s)$
K	equilibrium constant
K_j	adsorption constant for component j, atm^{-1}
L	tube length, m
N	total number of components (reaction side)
n_t	tube number
p_{H_2}	partial pressure of H_2, atm
Q_0	preexponetial factor in the Arrhenius relationship, mol/(s m $atm^{0.5}$)
r_{CO}	reaction rate, $mol_{CO}/(kg_{cat}\ s)$
P	pressure, atm
R	flow ratio = $\frac{F^P_{H_2,L}\cdot n_t}{F_{H_2,o}}$ (Fig. 8)
T	temperature, K
U	overall heat transfer coefficient, W/(m^2 K)
V	catalyst volume, cm^3
y	molar fraction of component
X	conversion
z	axial coordinate, m

Subscripts

cat	catalyst
j	component j
max	maximum
P	particle
T	total
te	external tube
ti	internal tube
o	at the axial coordinate $z=0$
L	at the axial coordinate $z=L$

Superscript

m	mean temperature
P	permeate
*	dimensionless

Greek letters

δ	thickness of the Pd layer, m
ΔH_r	heat of reaction, kJ/mol
ΔT_{ad}	adiabatic temperature rise, K
ρ_B	fixed-bed density, kg_{cat}/m^3

2. Mathematical model

A 1-D, pseudohomogeneous mathematical model has been selected to represent the steady-state operation of the multitubular membrane reactor [8]. The catalyst is packed in the shell (retentate side) while pure H_2 is collected inside the membrane tubes (permeate side) (Fig. 1).

The model considers the following hypotheses:

- isobaric conditions
- adiabatic shell (heat losses to environment are neglected)
- axial dispersion phenomena are neglected

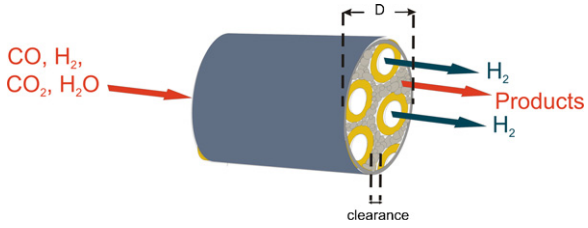

Fig. 1. Scheme of the multitubular membrane reactor.

- temperature and composition gradients in the radial coordinate are not considered
- ideal membrane, only H_2 permeates

The Langmiur–Hinshelwood kinetic model proposed by Podolski and Kim [9] is adopted in the simulations:

$$r_{CO} = \frac{kK_{CO}K_{H_2O}\left[P_{CO}P_{H_2O} - P_{CO_2}P_{H_2}/K\right]}{\left[1 + K_{CO}P_{CO} + K_{H_2O}P_{H_2O} + K_{CO_2}P_{CO_2}\right]^2} \quad (2)$$

The dependence on temperature of the rate constant (k), equilibrium constant (K) and adsorption constants (K_j) are presented in Table 1.

Under the aforementioned hypotheses, the mathematical model is the following:

Shell side (*catalyst*):

Mass balances

$$\frac{dF_{CO}}{dz} = A_T r_{CO}\rho_B \quad (3)$$

$$\frac{dF_{H_2}}{dz} = A_T(-r_{CO})\rho_B - \pi\, n_t d_{te} J_{H_2} \quad (4)$$

Energy balance

$$\frac{dT}{dz} = \frac{A_T\rho_B(-r_{CO})(-\Delta H_r) - \pi n_t d_{ti} U(T - T^P)}{\sum_{i=1}^{N} F_j C_{pj}} \quad (5)$$

Tube side (*permeate*):

Mass balance

$$\frac{dF^P}{dz} = (\pm)\pi\, d_{te} J_{H_2} \quad (6)$$

Table 1
The geometric parameters and operating conditions used for the simulations.

Design data	Feed conditions	Membrane properties
d_{ti} = 8 mm[a]	FT_0 = 345 mol/h (ca. 10 kWth)	Q_0 = 242 nmol/msPa$^{0.5}$[d]
d_{te} = 13.4 mm[a]	H_2 (%) = 43.48[b]	E = 16.3 kJ/mol
d_P = 1 mm	CO (%) = 7.97[b]	δ = 60 μm
V_{cat} = 2260 cm^3	CO_2 (%) = 10.99[b]	
n_t = 63[c]	CH_4 (%) = 5.68[b]	
	H_2O (%) = 31.88[b]	
	P = 10–20 atm	
	P^P = 1 atm	

Kinetic and equilibrium constants

$k = \exp\left(-\frac{14778.1}{T} + 20.292\right)$	$K_{CO} = \exp\left(\frac{1542.0}{T} - 3.392\right)$
$K_{H_2O} = \exp\left(-\frac{3128.3}{T} - 6.427\right)$	$K = \exp\left(\frac{4577.8}{T} - 4.33\right)$
	$K_{CO_2} = \exp\left(\frac{6312.0}{T} - 9.285\right)$

[a] Criscuoli et al. [11].
[b] Francesconi et al. [1].
[c] Adrover et al. [8].
[d] Barbieri et al. [10].

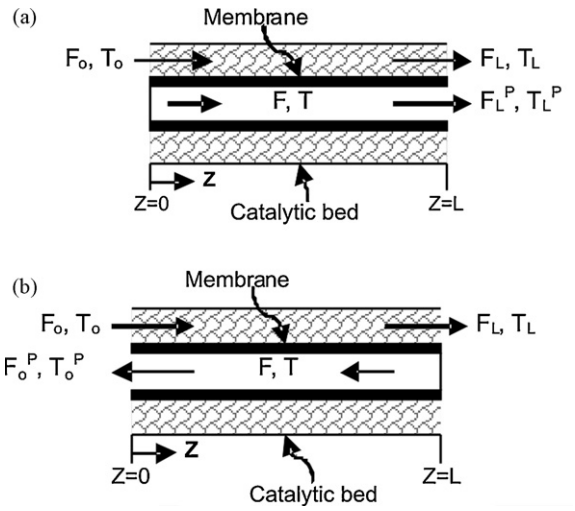

Fig. 2. (a) Cocurrent scheme and (b) countercurrent scheme.

Energy balance

$$\frac{dT^P}{dz} = (\pm)\frac{\pi d_{te}}{F^P_{H_2} C_{p_{H_2}}}\left[J_{H_2} C_{p_{H_2}} + U\frac{d_{ti}}{d_{te}}\right](T - T^P) \quad (7)$$

The molar flowrates of the remaining components are calculated using stoichiometric relationships. The signs (+) and (−) in Eqs. (6) and (7) correspond to cocurrent and countercurrent arrangements, respectively.

The boundary conditions for both configurations are the following (see Fig. 2):

Cocurrent

$$\text{At } z = 0: \begin{cases} F_j = F_{j,o} \text{ for } j = 1,\ 2...., N \\ T = T_o; T^P = T_o \\ F^P_{H_2} = 0; \end{cases} \quad (8)$$

Countercurrent

$$At\ z = 0: \begin{cases} F_j = F_{j,o} \text{ for } j = 1, 2...., N \\ T = T_o \end{cases} \quad (9)$$

$$At\ z = L: \begin{cases} F^P_{H_2} = 0 \\ T = T^P \end{cases} \quad (10)$$

It is worth mentioning that the cocurrent configuration leads to an initial value problem (IVP). Under this scheme, the H_2 flowrate in the permeate side is zero at $z = 0$ (Fig. 2a). Both temperatures (i.e., permeate and retentate side) are equal at $z = 0$ ($T_o = T^P_o$) because a small amount of H_2 permeates at the inlet temperature value. When the countercurrent configuration is chosen (Fig. 2b), the tubes are closed at $z = L$ and H_2 flows on the permeate side from $z = L$ to $z = 0$. By analogy with the cocurrent operation, the temperatures on both sides are equal at $z = L$ ($T_L = T^P_L$). This boundary value problem (BVP) is solved iteratively using the Shooting Method.

The permeation flowrate through the membrane is quantified by means of the Sieverts' Law [10]:

$$J_{H_2} = \frac{Q_0 e^{(-E/RT)}}{\delta}\left[\sqrt{p_{H_2}} - \sqrt{p^P_{H_2}}\right] \quad (11)$$

The global heat transfer coefficient (U) between retentate and permeate sides is assumed as a parameter. In this work, U takes similar values to those estimated by means of correlations, as described in [8]. It is important to highlight that the heat losses from the shell to the environment are neglected.

The geometric parameters and operating conditions used for the simulations are given in Table 1. The feed corresponds to a typical outlet stream of an ethanol reformer.

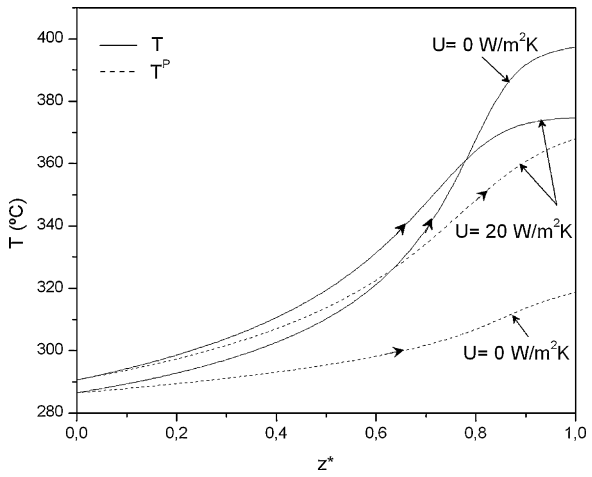

Fig. 3. Axial temperature profiles of retentate and permeate sides obtained at the same outlet conversion (X_{CO} = 95%). Cocurrent configuration.

3. Results and discussion

The behavior of the MR operating under cocurrent and countercurrent configurations is shown in Figs. 3 and 4, respectively. In both cases, inlet temperatures (T_o) have been chosen to achieve the same CO conversion (95%) at the reactor outlet. Two different values of the overall coefficient U are considered, namely $U = 0$ W/m² K and $U = 20$ W/m² K. Although the concept of the membrane being a perfect thermal insulator is strictly theoretical, it provides valuable information about the maximum temperature rise in the reaction side, particularly for the cocurrent operation. Besides, the value $U = 20$ W/m² K is similar to those predicted from correlations [8].

Fig. 3 shows that T^P augments axially even for the case $U = 0$, due to the H_2 permeation at progressively higher temperatures (T) towards the reactor outlet. When $U = 20$ W/m² K, the H_2 stream in the permeate side acts as a coolant medium, which tends to attenuate the temperature rise in the retentate side. As U increases, the temperature profiles corresponding to T and T^P approach each other. However, the relationship $T(z) \geq T^P(z)$ is always verified, even for very high values of U.

Analogous results are presented in Fig. 4 for the countercurrent flow scheme. The main difference with respect to Fig. 3 is that $T^P(z) \geq T(z)$, i.e. when U differs from zero the permeate stream acts as a heating medium of the reaction side. Fig. 4 also shows that as U increases, the outlet value of T^P (i.e., T^P_o) diminishes and the out-

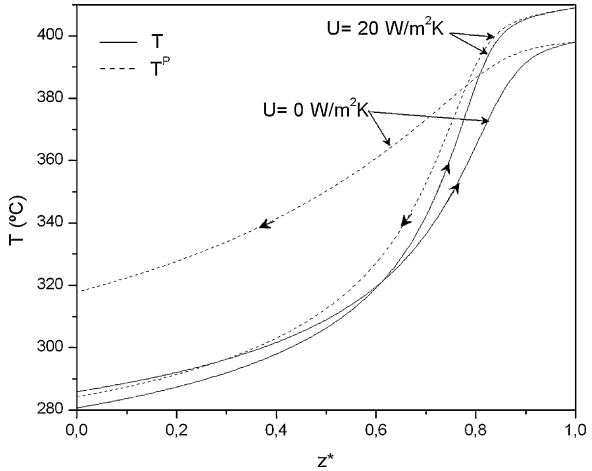

Fig. 4. Axial temperature profiles of retentate and permeate sides obtained at the same outlet conversion (X_{CO} = 95%). Countercurrent configuration.

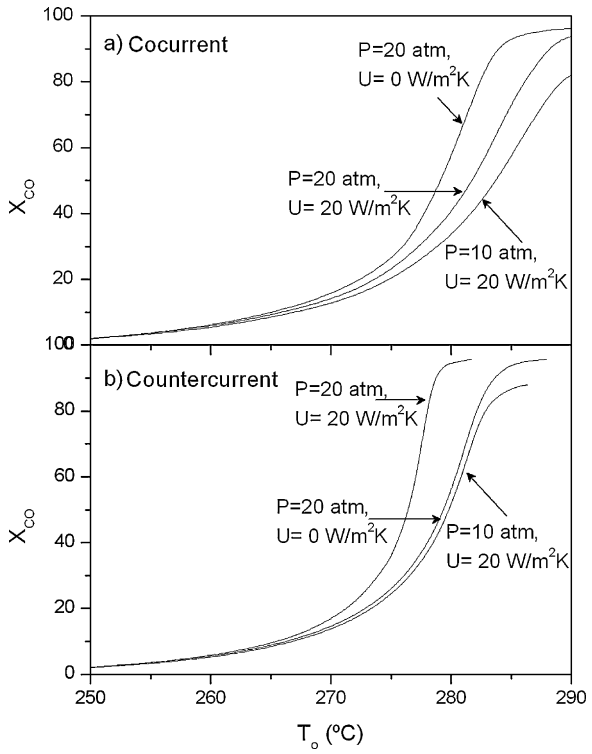

Fig. 5. Temperature-X_{CO} trajectories for different pressures and U values. (a) cocurrent and (b) countercurrent.

let value of T (i.e., T_L) increases, just the opposite of the cocurrent operation. When the coefficient $U \to \infty$, the temperature profiles $T(z)$ and $T^P(z)$ overlap, because of the high convective heat fluxes through the membrane. The overlaping is similar to that observed in the cocurrent operation. However, when a countercurrent configuration is selected, the total temperature rise for the catalyst side $(T_L - T_o)$ reaches its maximum.

Fig. 5 shows the influence of the feed temperature (T_o) on the outlet conversion of CO, for different values of the retentate pressure (P) and the heat transfer coefficient (U). Fig. 5a, corresponding to the cocurrent flow, shows that all the ignition curves present the characteristic sigmoid shape. As U increases the curves shift to the right, i.e., higher feed temperatures are needed for the same conversion level due to the cooling effect performed by the permeate stream, as explained in Fig. 3. For the countercurrent case (Fig. 5b), the ignition temperatures shift to the left as U increases. In other words, higher values of U contribute to a faster ignition of the reaction because the permeate stream acts as a heating medium and causes a partial feedback of the reaction heat.

Fig. 5 also includes curves corresponding to a lower value of the pressure in the shell side. For both flow configurations, lower total pressures in the catalyst side lead to higher ignition temperatures (compare curves for $P = 10$ atm and $P = 20$ atm). This effect can be attributed to the lower driven force for the permeation of H_2 through the membrane [6,8].

The ignition curves described above can be analyzed from a thermal point of view by quantifying the temperature rise (inlet–outlet) of the retentate and permeate streams. Fig. 6 shows these temperature increments for two values of the heat transfer coefficient for the cocurrent configuration. As T_o increases, the CO conversion augments (see Fig. 5a) and so does the total amount of heat generated by the reaction. This implies that the temperature rise at both the reaction side $(T_L - T_o)$ and the permeate side $(T_L^P - T_o)$ increases with the feed temperature, T_o. However, as already mentioned, an

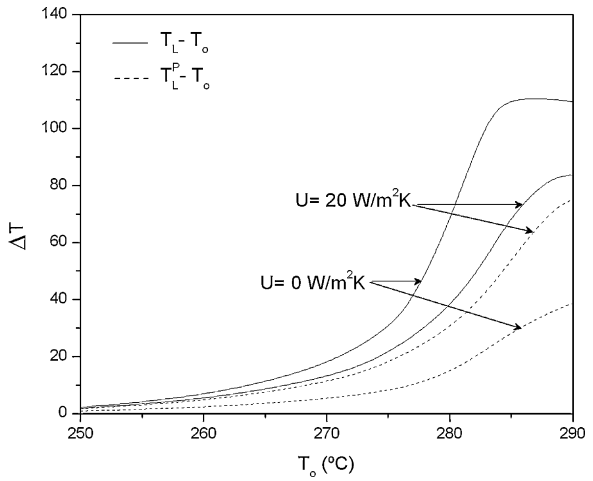

Fig. 6. $T_L - T_o$ and $T_L^P - T_o$ curves as a function of T_o, for different U values. Cocurrent configuration.

increase in the U value contributes to moderate the temperature increase in the catalyst bed $(T_L - T_o)$.

For high values of U, the temperature rise of both streams (retentate and permeate) tends to match, i.e.:

$$T_L - T_o \cong T_L^P - T_o = \Delta T_{ad} X_{CO} \tag{12}$$

where

$$\Delta T_{ad} = \frac{(-\Delta H_r) y_{CO,o}}{C_p} \tag{13}$$

is the adiabatic temperature rise of a conventional fixed-bed reactor.

Eq. (12) can be verified by means of the overall heat balance of the global unit. Thus, a heat balance between the reactor inlet $(z = 0)$ and any axial position leads to:

$$F_{CO,o} X_{CO} (-\Delta H_r) = F_{T,o} C_p^m (T - T_o) - n_t F_{H_2}^P C_{p_{H_2}}^m (T - T^P) \tag{14}$$

Rearranging Eq. (14) and evaluating it at the reactor outlet $(z = L)$ the following can be obtained:

$$T_L - T_o = \Delta T_{ad} X_{CO} + \left(\frac{n_t F_{H_2,L}^P}{F_{T,o}} \right) \left(\frac{C_{p_{H_2}}^m}{C_p^m} \right) \left(T_L - T_L^P \right) \tag{15}$$

Eq. (15) can be used to predict the temperature rise in the catalyst side of the membrane reactor when a cocurrent flow configuration is selected. It becomes clear that the temperature increase depends not only on the value of ΔT_{ad} and the conversion level, but also on the total permeated hydrogen/feed flowrate ratio and the difference between the outlet temperatures of both streams. Eq. (15) demonstrates that the MR leads to a higher temperature rise than the conventional FBR, even for the same outlet conversion (X_{CO}) [12].

At high values of the coefficient U, the outlet temperatures of both streams tend to coincide (i.e., $(T_L - T_L^P) \to 0$, see Fig. 3). Therefore, the second term of the right hand side of Eq. (15) vanishes, and Eq. (12) is verified. As a result, when the MR operates under cocurrent configuration and the heat exchange between both streams of the MR is highly efficient (high heat exchange areas per unit volume and heat transfer coefficients), the temperature rise in the MR can be calculated from the same equation used for the FBR (Eq. (13)). This equation establishes a linear relationship between the conversion and the increase of temperature on the catalyst side. Nevertheless, the actual temperature rise $(T_L - T_o)$ of the MR will be higher than that of the FBR because of the equilibrium shift caused by the membrane, which leads to higher CO conversions.

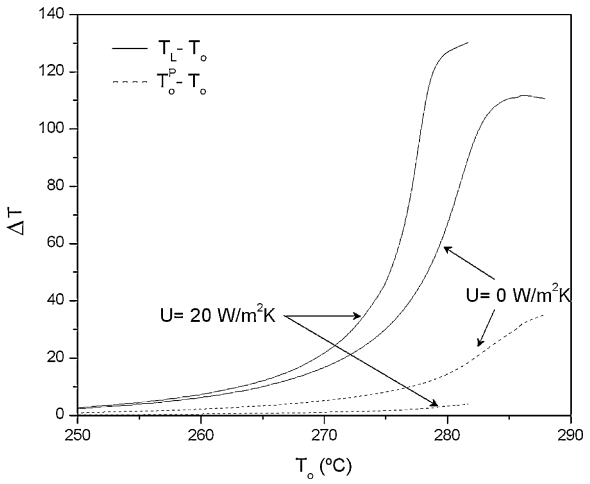

Fig. 7. $T_L - T_o$ and $T_o^P - T_o$ curves as a function of T_o, for different U values. Countercurrent configuration.

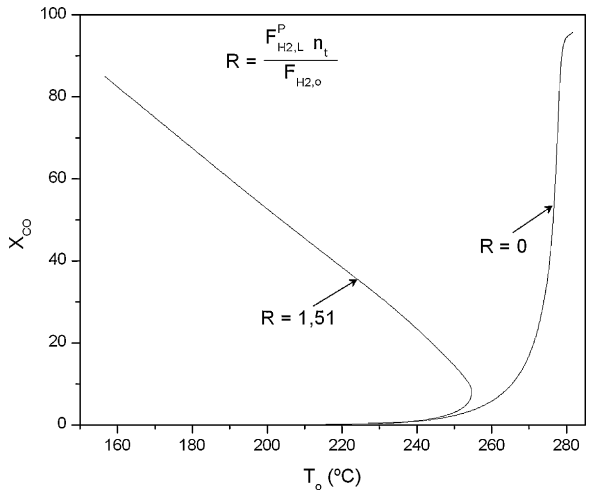

Fig. 8. Temperature-X_{CO} trajectories. Effect of the hydrogen fed as sweep gas in the permeate stream ($z = L$). Countercurrent configuration.

The scenario for the countercurrent flow configuration, however, is opposite. As shown in Fig. 7, as U increases the temperature rise in the reaction side ($T_L - T_o$) also increases. Conversely, the outlet temperature of the permeate stream (T_o^P) tends to approach the feed temperature (T_o) because of the heat transferred from the permeate stream to the retentate side (compare the dashed curves in Fig. 7). Under these conditions, the total temperature rise in the catalyst bed could exceed considerably the value given by Eq. (12).

This phenomenon can be explained from the overall heat balance for the countercurrent configuration. A heat balance between the inlet ($z = 0$) and the outlet ($z = L$) of the MR can be written as follows:

$$F_{CO,o}X_{CO}(-\Delta H_r) = F_{T,o}C_p^m(T_L - T_o) - n_t F_{H_2,o}^P C_{p_{H_2}}^m (T_L - T_o^P) \quad (16)$$

Rearranging Eq. (16):

$$T_L - T_o = \Delta T_{ad} X_{CO} + \left(\frac{n_t F_{H_2,o}^P}{F_{T,o}}\right)\left(\frac{C_{p_{H_2}}^m}{C_{p_{H_2}}^m}\right)(T_L - T_o^P) \quad (17)$$

Eq. (17) predicts the total temperature rise in the retentate side for the countercurrent scheme. The main difference between Eqs. (17) and (15) is that, for the same heat exchange area and the same U, the term $(T_L - T_o^P)$ (countercurrent) is considerably higher than $(T_L - T_L^P)$, corresponding to the cocurrent case. In addition, as the heat exchange between the permeate and retentate streams increases, the term $(T_L - T_o^P)$ in Eq. (17) tends to reach its maximum value, i.e.:

$$(T_L - T_o^P) \to (T_L - T_o) \quad (18)$$

Combining Eqs. (17) and (18):

$$(T_L - T_o)_{max} = \frac{\Delta T_{ad} X_{CO}}{1 - (n_t F_{H_2,o}^P / F_{T,o})(C_{p_{H_2}}^m / C_p^m)} \quad (19)$$

Eq. (19) predicts an upper bound for the temperature rise in a countercurrent membrane reactor.

Finally, it is important to mention that the countercurrent MR can exhibit steady-state multiplicity. This phenomenon was recently found in an MR with a sweep gas stream under countercurrent flow [13].

Fig. 8 shows the outlet CO conversion as a function of the feed temperature, for two different operating conditions under countercurrent flow. The curve corresponding to $R = 0$ is the same as the upper curve of Fig. 5b; clearly, the steady-state multiplicity phenomenon is not observed. Conversely, the curve corresponding to $R = 1.51$ represents a hypothetical membrane reactor where a given amount of H_2 is fed as "sweep gas" at the axial coordinate $z = L$. This additional H_2 flowrate ($F_{H_2,L}^P$), fed at temperature T_L, is assumed to be 1.51 times the H_2 flowrate in the feed stream, $F_{H_2,o}$. For this new operating condition, the countercurrent MR presents steady-state multiplicity; e.g., for $T_o = 250\,^\circ C$ at least two different steady-states exist.

For the operating conditions studied in this work, the countercurrent MR operating *without sweep gas* did not present steady-state multiplicity. However, unicity for other operating conditions cannot be guaranteed.

4. Conclusions

The comparison of the performance of the membrane reactor operating co- and countercurrently with the permeate stream leads to the following conclusions:

- The selected flow configuration has an important influence on the thermal behavior of the MR.
- The cocurrent scheme attenuates the thermal effects in the MR by minimizing the temperature rise in the catalyst bed. This favorable effect is a consequence of the heat exchange with the permeate stream, which acts as a cooling medium along the reactor length.
- Although the countercurrent configuration facilitates the reaction ignition due to the preheating effect caused by the permeate stream, this flow scheme can lead to high temperature rises along the axial position. These high temperature rises can exceed considerably the value of ΔT_{ad}. The heat feedback, which is inherent in any countercurrent heat exchange, is a source of instability that could lead to conditions of steady-state multiplicity.
- The temperature rise of both the cocurrent and countercurrent MRs can be calculated from simple algebraic expressions (Eqs. (15) and (17)) derived from the overall heat balances. It is important to note that the cocurrent MR can operate on the same linear trajectory as a conventional adiabatic FBR (Eq. (12)), provided that an efficient heat exchange between the two internal streams of the MR occurs.

References

[1] J.A. Francesconi, M.C. Mussati, P. Aguirre, J. Power Sources 173 (2007) 467.
[2] T.P. Tiemersma, C.S. Patil, M. van Sint Annaland, J.A.M. Kuipers, Chem. Eng. Sci. 61 (2006) 1602.
[3] B.N. Lukyanov, D.V. Andreev, V.N. Parmon, Chem. Eng. J 154 (1–3) (2009) 258.

[4] M. De Falco, P. Nardella, L. Marrelli, L. Di Paola, A. Basile, F. Gallucci, Chem. Eng. J. 138 (2008) 442.
[5] M. Koukou, G. Chaloulou, N. Papayannakos, N. Markatos, Int. J. Heat Mass Tranf. 40 (1997) 2407.
[6] A. Brunetti, A. Caravella, G. Barbieri, E. Drioli, J. Membr. Sci. 306 (2007) 329.
[7] A. Basile, L. Paturzo, F. Gallucci, Catal. Tod. 82 (2003) 275.
[8] M.E. Adrover, E. López, D. Borio, M. Pedernera, Chem. Eng. J. 154 (1–3) (2009) 196.
[9] W.F. Podolski, Y.G. Kim, Ind. Eng. Chem. 13 (4) (1974) 415.
[10] G. Barbieri, A. Brunetti, T. Granato, P. Bernardo, E. Drioli, Ind. Eng. Chem. Res. 44 (2005) 7676.
[11] A. Criscuoli, A. Basile, E. Drioli, Catal. Tod. 56 (2000) 53.
[12] M.E. Adrover, E. López, M.N. Pedernera, D.O. Borio, Stud. Surf. Sci. Catal. 167 (2007) 83.
[13] M.E. Adrover, E. López, D.O. Borio, M.N. Pedernera, AIChE J 55 (12) (2009) 3206.